CAUCHY – Jurnal Matematika Murni dan Aplikasi
Volume 11 (2) (2026), Pages 2532–2549
p-ISSN: 2086-0382; e-ISSN: 2477-3344

Dynamic Analysis of Three-Species System with Fear Effect on Prey and Allee Effect on Top Predator

Dana Eky Novya and Dian Savitri*

Department of Mathematics, Faculty of Mathematics and Natural Sciences, Universitas Negeri Surabaya, Indonesia

Abstract

Fear-induced behavioral responses and low-density reproductive limitations can affect the stability and persistence of interacting populations. This study investigates a three-species system consisting of prey, middle predator, and top predator, incorporating a fear effect on prey growth and an Allee effect on top predator reproduction. The existence and local stability of biologically feasible equilibria are analyzed using the Jacobian matrix and Routh–Hurwitz criterion. Numerical continuation with MATCONT is employed to identify bifurcations associated with ecological and predation parameters, while numerical simulations are performed using the adaptive fourth–fifth-order Runge–Kutta method. For the selected parameter set, two positive coexistence equilibria are obtained, with the first unstable and the second locally asymptotically stable. The continuation analysis reveals limit-point bifurcations for both the Allee-effect and fear-effect parameters. Further analysis shows that variation in the middle-predator predation rate m_1 produces two limit-point bifurcations, whereas variation in the top-predator predation rate m_2 generates one limit point and a subcritical Hopf bifurcation. The latter indicates the emergence of an unstable periodic orbit near $m_2 = 2.232969$. Numerical simulations confirm convergence toward the stable coexistence equilibrium with damped oscillatory transients. These results demonstrate that fear, Allee effects, and predation rates can alter the number and stability of coexistence equilibria and induce both equilibrium and oscillatory transitions in the three-species system.

Keywords: Allee effect; bifurcation analysis; fear effect; local stability; three-species system

Copyright © 2026 by Authors, Published by CAUCHY Group. This is an open access article under the CC BY-SA License (https://creativecommons.org/licenses/by-sa/4.0)

1. Introduction

Mathematical models of interacting populations provide a useful framework for studying population persistence, coexistence, and stability. In predator–prey systems, population dynamics are governed not only by direct trophic interactions but also by behavioral responses and density-dependent demographic effects. One important behavioral mechanism is the fear effect, whereby predator presence alters prey behavior and reproduction, thereby modifying prey growth [1, 2]. Its inclusion can substantially affect equilibrium stability and temporal dynamics [1, 3].

Fear effects have also been incorporated into multi-species food-chain models. Cong et al. [2] studied a three-species food-chain model with predator-induced fear, while Pal et al. [4] examined fear effects in a three-species food chain with a generalist predator. These studies

*Corresponding author. E-mail: diansavitri@unesa.ac.id

Received: September 2, 2026 Revised: October 22, 2026 Accepted: October 27, 2026
DOI: https://doi.org/10.18860/cauchy.v11i2.45901

demonstrate that behavioral responses at one trophic level can propagate through the food chain and alter the dynamics of interacting populations.

Another mechanism affecting population persistence is the Allee effect, which describes reduced population performance at low density. It may arise from limitations in reproduction, mating, or other low-density processes and can alter the existence and stability of population equilibria [5, 6]. In food-chain models, Allee effects can influence the persistence and stability of interacting populations [7]. In particular, component Allee effects in predator reproduction provide a density-dependent mechanism linking predator persistence to its own population density [6].

The combined influence of fear and Allee effects has also been investigated in several ecological models. Lai et al. [8] analyzed stability and bifurcation in a predator–prey model incorporating an additive Allee effect and fear, while Xie [3] examined their interaction in a Holling type-II predator–prey system. Ratio-dependent and spatiotemporal formulations have further shown that the interaction between these mechanisms can modify equilibrium and bifurcation structures [9, 10]. For three-species food chains, Rana et al. [11] investigated the combined effects of fear and Allee mechanisms and their resulting complex dynamics.

More recently, Kumar et al. [12] considered a three-species food-chain model in which fear affects the bottom prey and the Allee effect acts on the top predator, making it particularly close to the present study. However, the mathematical formulations are different. Kumar et al. [12] employed saturating Holling type-II functional responses for the trophic interactions, whereas the present model uses bilinear interactions, m_1xy and m_2yz. Moreover, the Allee effect in the present model enters the top-predator growth term through the multiplicative factor $z/(\gamma + z)$. Therefore, the contribution of the present study is not simply the combination of fear and Allee effects, which has already been investigated, but the analysis of the equilibrium and bifurcation consequences generated by this specific nonlinear formulation.

The proposed formulation leads to a nontrivial coexistence structure. In particular, the equilibrium relations can yield multiple positive coexistence equilibria with different local stability properties. Under the parameter set considered in this study, two positive coexistence equilibria are obtained, with one being unstable and the other locally asymptotically stable. This equilibrium multiplicity provides a direct connection between the specific nonlinear interactions in the model and the resulting coexistence dynamics.

Furthermore, a systematic one-parameter continuation is performed with respect to four ecologically relevant parameters: the fear parameter α, the Allee parameter γ, the middle-predator predation rate m_1, and the top-predator predation rate m_2. The continuation analysis identifies a limit-point bifurcation along the α continuation, a limit-point bifurcation along the γ continuation, two distinct limit points along the m_1 continuation, and both a limit point and a Hopf bifurcation along the m_2 continuation. Thus, the analysis characterizes how the specific fear, Allee, and trophic-interaction parameters affect the equilibrium structure and local dynamics of the proposed system.

In this study, we consider a three-species system consisting of prey (x), middle predator (y), and top predator (z). The prey experiences a fear effect that reduces its effective growth rate through the density-dependent factor $1/(1 + \alpha y)$, where α measures the intensity of predator-induced fear. The top predator is subject to an Allee effect represented by $z/(\gamma + z)$, where γ is the Allee-effect parameter. The resulting system is investigated in terms of positivity and boundedness, equilibrium existence, local stability, and bifurcation structure.

The objective of this study is therefore to determine how the specific nonlinear formulation of fear, Allee, and bilinear trophic interactions shapes coexistence and local stability in the three-species system. The positive coexistence equilibria are characterized analytically, while numerical continuation is employed to identify limit-point and Hopf bifurcations associated with α, γ, m_1, and m_2. Numerical simulations are subsequently used to illustrate the resulting population dynamics and complement the local stability analysis. The study thereby provides a

focused characterization of the equilibrium multiplicity and bifurcation structure generated by the proposed mathematical formulation.

2. Methods

The proposed system was analyzed using numerical integration and continuation to verify the analytical results and characterize its dynamics and bifurcations.

2.1. Numerical Integration and Stability Verification

The system in Eq. (1) was integrated in Python using `solve_ivp` with adaptive RK45, rtol $= 10^{-9}$, and atol $= 10^{-11}$. Time-series and phase-space simulations used $0 \leq t \leq 40$ and $0 \leq t \leq 150$, respectively, with 5000 equally spaced evaluation points. Positive initial conditions were used, with single and multiple conditions for the respective simulations.

2.2. Bifurcation Analysis and Numerical Continuation

One-parameter continuation was performed in MATCONT within MATLAB by varying γ, α, m_1, and m_2 individually while fixing the remaining parameters. Predictor–corrector continuation with adaptive step sizes of 0.01, 10^{-5}, and 0.1 (initial, minimum, and maximum), adaptation parameter 3, and 300 maximum points was used. Newton correction employed 3 Newton iterations, 10 correction iterations, and 10 test iterations, with variable/function tolerances 10^{-6}, test tolerance 10^{-5}, and Jacobian increment 10^{-5}; TSearch order and Moore–Penrose options were enabled. LPs were identified by a simple zero eigenvalue and verified using the quadratic normal-form coefficient, while Hopf points were identified by a purely imaginary eigenvalue pair and characterized using the first Lyapunov coefficient.

3. Results and Discussion

The analysis begins with the formulation of the three-species model. Positivity, boundedness, equilibrium existence, and local stability are then examined. Numerical simulations and bifurcation analysis illustrate the resulting dynamics and the effects of varying the model parameters.

3.1. Mathematical Model Formulation

We consider three interacting populations: prey (x), middle predator (y), and top predator (z). The prey grows logistically with intrinsic birth rate b, competition coefficient a, and mortality rate d, while the middle predator consumes the prey linearly with predation rate m_1 and efficiency e_1, and the top predator consumes the middle predator with rate m_2 and efficiency e_2, with natural mortalities d_1 and d_2, respectively. The middle predator induces a *fear effect* on the prey by reducing its birth rate through $1/(1+\alpha y)$, where α measures fear intensity. Meanwhile, the top predator experiences an *Allee effect* due to mating limitations at low densities, represented by $z/(\gamma+z)$, where γ measures the Allee effect strength. Based on these assumptions, the system is formulated as the following nonlinear autonomous ordinary differential equations:

$$\begin{aligned}
\frac{dx}{dt} &= \frac{bx}{1+\alpha y} - ax^2 - dx - m_1 xy, \\
\frac{dy}{dt} &= e_1 m_1 xy - d_1 y - m_2 yz, \\
\frac{dz}{dt} &= e_2 m_2 yz \left(\frac{z}{\gamma+z}\right) - d_2 z,
\end{aligned} \tag{1}$$

The model is considered in generic population and time units rather than being calibrated to a specific ecological food chain. Accordingly, the parameter values are interpreted within the mathematical scaling of the model and are used to illustrate the dynamical behavior of the system

rather than to provide quantitative predictions for a specific ecological population. All model parameters are positive, with $0 < e_1, e_2 \leq 1$. These assumptions are used in the boundedness analysis. The system is subject to the initial conditions $x(0) > 0$, $y(0) > 0$, and $z(0) > 0$. All parameters utilized in the system in Eq. (1) are assumed to be strictly positive, as summarized in Table 1.

Table 1: Ecological descriptions of the model parameters.

Parameter	Biological Description
b	Intrinsic birth rate of the prey
a	Intraspecific competition rate of the prey
d	Natural death rate of the prey
α	Intensity of the fear effect induced by the middle predator
m_1	Predation rate of the middle predator on the prey
e_1	Biomass conversion efficiency of the middle predator
d_1	Natural death rate of the middle predator
m_2	Predation rate of the top predator on the middle predator
e_2	Biomass conversion efficiency of the top predator
γ	Allee-effect scale parameter (mating limitation)
d_2	Natural death rate of the top predator

3.2. Positivity and Boundedness

Let $x(0), y(0), z(0) > 0$. The system in Eq. (1) can be written as

$$\begin{aligned}
\dot{x} &= x\left(\frac{b}{1+\alpha y} - ax - d - m_1 y\right), \\
\dot{y} &= y\left(e_1 m_1 x - d_1 - m_2 z\right), \\
\dot{z} &= z\left(e_2 m_2 y \frac{z}{\gamma + z} - d_2\right).
\end{aligned}$$

Since each equation contains its corresponding population variable as a factor, the coordinate planes are invariant. Hence, $\mathbb{R}^3_+$ is positively invariant and $x(t), y(t), z(t) \geq 0$ for all $t \geq 0$. To prove boundedness, define $N = x + y + z$. Under the assumptions $0 < e_1, e_2 \leq 1$ and $a, d, d_1, d_2 > 0$, summing the three equations gives

$$\begin{aligned}
\dot{N} = \frac{bx}{1+\alpha y} - ax^2 - dx + (e_1 - 1)m_1 xy - d_1 y \\
- m_2 yz + e_2 m_2 yz \frac{z}{\gamma + z} - d_2 z.
\end{aligned}$$

The interaction terms involving m_2 can be written exactly as

$$-m_2 yz + e_2 m_2 yz \frac{z}{\gamma + z} = (e_2 - 1)m_2 yz \frac{z}{\gamma + z} - \frac{\gamma m_2 yz}{\gamma + z}.$$

Since $0 < e_1, e_2 \leq 1$, both interaction contributions are non-positive. Moreover,

$$\frac{bx}{1+\alpha y} \leq bx$$

and

$$bx - ax^2 \leq \frac{b^2}{4a}.$$

Therefore,

$$\dot{N} \leq \frac{b^2}{4a} - dx - d_1 y - d_2 z.$$

Let

$$\delta = \min\{d, d_1, d_2\} > 0.$$

Since

$$dx + d_1 y + d_2 z \geq \delta(x + y + z) = \delta N,$$

we obtain

$$\dot{N} \leq \frac{b^2}{4a} - \delta N.$$

By the comparison theorem,

$$N(t) \leq N(0)e^{-\delta t} + \frac{b^2}{4a\delta}\left(1 - e^{-\delta t}\right).$$

Thus,

$$\limsup_{t\to\infty} N(t) \leq \frac{b^2}{4a\delta},$$

so all nonnegative solutions are bounded. Therefore, under the stated assumptions, the system in Eq. (1) is positively invariant and bounded in $\mathbb{R}^3_+$.

3.3. Existence and Stability Analysis of Equilibrium Points

The steady states of the proposed three-species system are evaluated to determine the possible population states of the model. The equilibrium points are obtained by setting the temporal derivatives in the system in Eq. (1) equal to zero, which gives the following algebraic system:

$$\begin{aligned} \frac{bx}{1+\alpha y} - ax^2 - dx - m_1 xy &= 0, \\ e_1 m_1 xy - d_1 y - m_2 yz &= 0, \\ e_2 m_2 yz\left(\frac{z}{\gamma + z}\right) - d_2 z &= 0. \end{aligned} \tag{2}$$

From the nonlinear algebraic system in Eq. (2), the equilibrium points and their corresponding existence conditions are obtained as follows.

1. The trivial equilibrium point

   $$E_0 = (0, 0, 0),$$

   which always exists and represents the extinction of all populations.
2. The prey-only equilibrium point

   $$E_1 = (x_1^*, 0, 0).$$

   Setting $y = 0$ and $z = 0$ in the first equation of Eq. (2) gives

   $$x_1^* = \frac{b - d}{a}.$$

   Thus, the axial equilibrium E_1 is biologically feasible when the condition in Eq. (3) holds:

   $$b > d. \tag{3}$$

3. The planar top-predator-free equilibrium branches are obtained by setting $z = 0$ while maintaining $x > 0$ and $y \neq 0$. From the second equation of Eq. (2),

   $$e_1 m_1 xy - d_1 y = 0.$$

For $y \neq 0$, it follows that

$$x_2^* = x_3^* = \frac{d_1}{e_1 m_1}.$$

Substituting this expression into the first equation of Eq. (2) and multiplying by $1 + \alpha y$ gives the quadratic equation in Eq. (4)

$$(m_1^2 \alpha e_1) y^2 + \left[a\alpha d_1 + d\alpha e_1 m_1 + m_1^2 e_1 \right] y + [a d_1 + d e_1 m_1 - b e_1 m_1] = 0. \tag{4}$$

Let

$$A = m_1^2 \alpha e_1 > 0,$$

$$B = a\alpha d_1 + d\alpha e_1 m_1 + m_1^2 e_1 > 0,$$

and

$$C = a d_1 + d e_1 m_1 - b e_1 m_1.$$

Then Eq. (4) becomes

$$A y^2 + B y + C = 0.$$

The two algebraic roots are

$$y_{2,3}^* = \frac{-B \pm \sqrt{\Delta}}{2A}, \qquad \Delta = B^2 - 4AC.$$

For a biologically feasible planar equilibrium, $y > 0$ is required. Since $A > 0$ and $B > 0$, the condition $C < 0$ implies that the two roots have opposite signs. The condition $C < 0$ is equivalent to

$$b > d + \frac{a d_1}{e_1 m_1}. \tag{5}$$

Hence, under the condition in Eq. (5), exactly one root is positive and defines the biologically feasible planar equilibrium

$$E_2 = (x_2^*, y_2^*, 0),$$

where

$$x_2^* = \frac{d_1}{e_1 m_1}, \qquad y_2^* > 0.$$

The other root satisfies $y_3^* < 0$ and therefore lies outside the biologically relevant region $\mathbb{R}_+^3$. Thus, E_3 is retained only as a nonphysical algebraic branch and is excluded from the subsequent biological stability analysis.

4. The positive interior coexistence equilibria
For the positive interior equilibrium, let $E_4 = (x^*, y^*, z^*)$, with $x^* > 0$, $y^* > 0$, and $z^* > 0$. From the third equation of Eq. (2), assuming $z^* \neq 0$, we obtain the expression for z^* in Eq. (6):

$$z^* = \frac{d_2 \gamma}{e_2 m_2 y^* - d_2}, \qquad y^* > \frac{d_2}{e_2 m_2}. \tag{6}$$

From the first equation of Eq. (2), since $x^* > 0$, it follows that

$$\frac{b}{1 + \alpha y^*} - a x^* - d - m_1 y^* = 0,$$

which yields the expression for x^* in Eq. (7):

$$x^* = \frac{1}{a} \left[\frac{b}{1 + \alpha y^*} - d - m_1 y^* \right]. \tag{7}$$

Thus, the positivity of x^* requires

$$\frac{b}{1+\alpha y^*} > d + m_1 y^*.$$

Alternatively, from the second and third equilibrium equations, x^* and y^* can be expressed in terms of z^* as

$$x^* = \frac{d_1 + m_2 z^*}{e_1 m_1}, \tag{8}$$

and

$$y^* = \frac{d_2(\gamma + z^*)}{e_2 m_2 z^*}. \tag{9}$$

Substituting Eq. (8) and Eq. (9) into the first equilibrium equation yields the reduced scalar equation

$$G(z^*) = \frac{b}{1+\alpha y^*} - a x^* - d - m_1 y^* = 0, \tag{10}$$

where x^* and y^* are given by Eq. (8) and Eq. (9), respectively. Each positive root z^* that generates positive values of x^* and y^* corresponds to a biologically feasible coexistence equilibrium. To identify these equilibria, Eq. (10) was initially solved over $10^{-4} \leq z^* \leq 10^3$ using a logarithmically spaced grid of 20,000 points and Brent's method on intervals exhibiting sign changes. However, a sign-change-based search alone may fail to detect tangential or even-multiplicity roots. Therefore, to further verify the completeness of the root search, the reduced equation was also transformed into an equivalent cubic polynomial, and all its roots were examined.
For the parameter set used in the numerical simulations, the resulting polynomial is

$$H(z) = -0.355z^3 + 2.57888z^2 - 0.80724z - 0.14112 = 0. \tag{11}$$

Solving Eq. (11) yields three distinct real roots, approximately

$$\begin{aligned} z_1 &= 0.460978876536, \\ z_2 &= 6.927944718532, \\ z_3 &= -0.124472890843. \end{aligned}$$

The first two roots are positive and yield biologically feasible coexistence equilibria, whereas the third root is negative and therefore biologically infeasible. Furthermore, evaluating $H(z)$ at its critical points gives nonzero values, confirming that neither critical point is a repeated root for the parameter set used in the numerical simulations.
Substituting the two positive roots into the expressions for the equilibrium components yields the two biologically feasible coexistence equilibria. The first equilibrium, $E_{4,1}$, is given in Eq. (12), whereas the second equilibrium, $E_{4,2}$, is given in Eq. (13):

$$E_{4,1} = (2.30691511,\ 8.87403103,\ 0.46097888), \tag{12}$$

$$E_{4,2} = (11.28881211,\ 3.20416027,\ 6.92794472). \tag{13}$$

Both equilibria have positive components and are therefore biologically feasible. Both equilibria belong to the biologically feasible region $\mathbb{R}^3_+$. The polynomial-root analysis confirms that these are the only biologically feasible positive interior equilibria for the specified parameter set. Their coexistence under the same parameter values indicates the possibility of multiple interior equilibrium states; the existence of a limit-point bifurcation, however, requires separate bifurcation analysis.

Now, we study the local stability of the dynamic system in Eq. (1) around each equilibrium point. The Jacobian matrix of the system in Eq. (1) is

$$J(x,y,z) = \begin{pmatrix} \dfrac{b}{1+\alpha y} - 2ax - d - m_1 y & -\dfrac{b\alpha x}{(1+\alpha y)^2} - m_1 x & 0 \\ e_1 m_1 y & e_1 m_1 x - d_1 - m_2 z & -m_2 y \\ 0 & \dfrac{e_2 m_2 z^2}{\gamma + z} & \dfrac{e_2 m_2 yz(2\gamma + z)}{(\gamma + z)^2} - d_2 \end{pmatrix}.$$

By evaluating the Jacobian matrix at each equilibrium point, the local stability properties of the equilibria are obtained as follows.

Theorem 1. *The total extinction equilibrium point $E_0 = (0,0,0)$ is locally asymptotically stable if $b < d$, and is unstable if $b > d$.*

Proof. The Jacobian matrix evaluated at E_0 is

$$J(E_0) = \begin{pmatrix} b-d & 0 & 0 \\ 0 & -d_1 & 0 \\ 0 & 0 & -d_2 \end{pmatrix}.$$

The characteristic equation is

$$(\lambda - (b-d))(\lambda + d_1)(\lambda + d_2) = 0.$$

Therefore, the eigenvalues are

$$\lambda_1 = b - d, \qquad \lambda_2 = -d_1, \qquad \lambda_3 = -d_2.$$

Since $d_1 > 0$ and $d_2 > 0$, the second and third eigenvalues are always negative. Thus, if $b < d$, all eigenvalues have negative real parts and E_0 is locally asymptotically stable. Conversely, if $b > d$, then $\lambda_1 > 0$, so E_0 is unstable. At the threshold value $b = d$, one eigenvalue is zero and the equilibrium is non-hyperbolic. □

Theorem 2. *The axial predator-free fixed point E_1 of the system is locally asymptotically stable if*

$$b > d$$

and

$$d_1 > \frac{e_1 m_1 (b-d)}{a}.$$

Proof. The Jacobian matrix evaluated at equilibrium point E_1 is

$$J(E_1) = \begin{pmatrix} -(b-d) & -\dfrac{b\alpha(b-d)}{a} - \dfrac{m_1(b-d)}{a} & 0 \\ 0 & \dfrac{e_1 m_1 (b-d)}{a} - d_1 & 0 \\ 0 & 0 & -d_2 \end{pmatrix}.$$

The eigenvalues associated with the Jacobian matrix $J(E_1)$ are

$$\lambda_1 = -(b-d),$$

$$\lambda_2 = \frac{e_1 m_1 (b-d)}{a} - d_1,$$

and

$$\lambda_3 = -d_2.$$

Since $\lambda_1 < 0$ under $b > d$ and $\lambda_3 = -d_2 < 0$, the stability of E_1 depends on $\lambda_2 < 0$. Therefore,

$$d_1 > \frac{e_1 m_1 (b-d)}{a}$$

ensures that all eigenvalues have negative real parts. Hence, E_1 is locally asymptotically stable under the stated conditions. □

Proposition 1. *Under the existence condition in Eq. (5), the two algebraic roots of the planar equilibrium equation have opposite signs. Hence, the equilibrium E_2 corresponds to the unique biologically feasible planar equilibrium, whereas E_3 lies outside the biological region $\mathbb{R}^3_+$.*

Theorem 3. *The biologically feasible planar top-predator-free equilibrium*

$$E_2 = (x_2^*, y_2^*, 0)$$

is locally asymptotically stable whenever it exists.

Proof. At the planar equilibrium $E_2 = (x_2^*, y_2^*, 0)$, the Jacobian matrix has the block-triangular form

$$J(E_2) = \begin{pmatrix} J_{11} & J_{12} & 0 \\ J_{21} & J_{22} & J_{23} \\ 0 & 0 & -d_2 \end{pmatrix},$$

where

$$\begin{aligned} J_{11} &= \frac{b}{1+\alpha y_2^*} - 2a x_2^* - d - m_1 y_2^*, \\ J_{12} &= -\frac{b\alpha x_2^*}{(1+\alpha y_2^*)^2} - m_1 x_2^*, \\ J_{21} &= e_1 m_1 y_2^*, \\ J_{22} &= e_1 m_1 x_2^* - d_1, \\ J_{23} &= -m_2 y_2^*. \end{aligned}$$

Since

$$x_2^* = \frac{d_1}{e_1 m_1},$$

we have

$$J_{22} = e_1 m_1 \left(\frac{d_1}{e_1 m_1} \right) - d_1 = 0.$$

Moreover, because E_2 satisfies the first equilibrium equation,

$$\frac{b}{1+\alpha y_2^*} - d - m_1 y_2^* = a x_2^*.$$

Therefore,

$$J_{11} = \frac{b}{1+\alpha y_2^*} - 2ax_2^* - d - m_1 y_2^* = -ax_2^* < 0.$$

The third eigenvalue is

$$\lambda_3 = -d_2 < 0.$$

The remaining two eigenvalues are determined by the upper-left 2×2 block, whose characteristic polynomial is

$$\lambda^2 + A_1\lambda + A_2 = 0,$$

where

$$A_1 = -J_{11} = ax_2^* > 0$$

and

$$A_2 = -J_{12}J_{21}.$$

Since

$$J_{12} = -\frac{b\alpha x_2^*}{(1+\alpha y_2^*)^2} - m_1 x_2^* < 0$$

and

$$J_{21} = e_1 m_1 y_2^* > 0,$$

we obtain

$$A_2 = -J_{12}J_{21} > 0.$$

Thus, by the Routh–Hurwitz criterion for a second-order polynomial, both eigenvalues associated with the upper-left 2×2 block have negative real parts. Together with

$$\lambda_3 = -d_2 < 0,$$

all eigenvalues of $J(E_2)$ have negative real parts. Hence, the planar top-predator-free equilibrium E_2 is locally asymptotically stable whenever it exists. □

Theorem 4. *Let $E_4 = (x^*, y^*, z^*)$, $x^*, y^*, z^* > 0$, be a biologically feasible positive coexistence equilibrium of the system in Eq. (1). Then E_4 is locally asymptotically stable if the coefficients of $\lambda^3 + a_1\lambda^2 + a_2\lambda + a_3 = 0$ satisfy $a_1 > 0$, $a_2 > 0$, $a_3 > 0$, $a_1 a_2 > a_3$, where the coefficients are given by the model-specific expressions below.*

Proof. At E_4, the Jacobian is

$$J(E_4) = \begin{pmatrix} J_{11} & J_{12} & 0 \\ J_{21} & J_{22} & J_{23} \\ 0 & J_{32} & J_{33} \end{pmatrix},$$

where

$$\begin{aligned} J_{11} &= \frac{b}{1+\alpha y^*} - 2ax^* - d - m_1 y^*, \\ J_{12} &= -\frac{b\alpha x^*}{(1+\alpha y^*)^2} - m_1 x^*, \\ J_{21} &= e_1 m_1 y^*, \\ J_{22} &= e_1 m_1 x^* - d_1 - m_2 z^*, \\ J_{23} &= -m_2 y^*, \end{aligned}$$

$$J_{32} = \frac{e_2 m_2 (z^*)^2}{\gamma + z^*},$$
$$J_{33} = \frac{e_2 m_2 y^* z^* (2\gamma + z^*)}{(\gamma + z^*)^2} - d_2.$$

From the first and second equilibrium equations,

$$\frac{b}{1+\alpha y^*} - a x^* - d - m_1 y^* = 0, \qquad e_1 m_1 x^* - d_1 - m_2 z^* = 0.$$

Thus,

$$J_{11} = -a x^* < 0, \qquad J_{22} = 0.$$

Consequently, the characteristic coefficients reduce to

$$a_1 = a x^* - J_{33}, \tag{14}$$
$$a_2 = -a x^* J_{33} - J_{12} J_{21} - J_{23} J_{32}, \tag{15}$$
$$a_3 = -a x^* J_{23} J_{32} + J_{12} J_{21} J_{33}. \tag{16}$$

Using the Jacobian entries, the coefficients a_2 and a_3 are obtained as given in Eq. (17) and Eq. (18), respectively:

$$a_2 = -a x^* J_{33} + \left[\frac{b\alpha x^*}{(1+\alpha y^*)^2} + m_1 x^*\right] e_1 m_1 y^* + \frac{e_2 m_2^2 y^* (z^*)^2}{\gamma + z^*}, \tag{17}$$

$$a_3 = \frac{a e_2 m_2^2 x^* y^* (z^*)^2}{\gamma + z^*} - \left[\frac{b\alpha x^*}{(1+\alpha y^*)^2} + m_1 x^*\right] e_1 m_1 y^* J_{33}. \tag{18}$$

Here,

$$-J_{12} J_{21} > 0, \qquad -J_{23} J_{32} = \frac{e_2 m_2^2 y^* (z^*)^2}{\gamma + z^*} > 0,$$

so the prey–middle-predator and middle-predator–top-predator couplings contribute positively to a_2, whereas J_{33} contains the top-predator self-dynamics and the Allee-effect parameter γ. By the Routh–Hurwitz criterion for a cubic polynomial, all eigenvalues have negative real parts if and only if

$$a_1 > 0, \qquad a_2 > 0, \qquad a_3 > 0, \qquad a_1 a_2 > a_3.$$

These conditions are therefore evaluated separately at each positive coexistence equilibrium, allowing $E_{4,1}$ and $E_{4,2}$ to have different local stability properties. □

The stability of each biologically feasible positive coexistence equilibrium is determined independently using the model-specific coefficients in Eq. (14)–Eq. (16) and the Routh–Hurwitz conditions.

3.4. Numerical Simulations

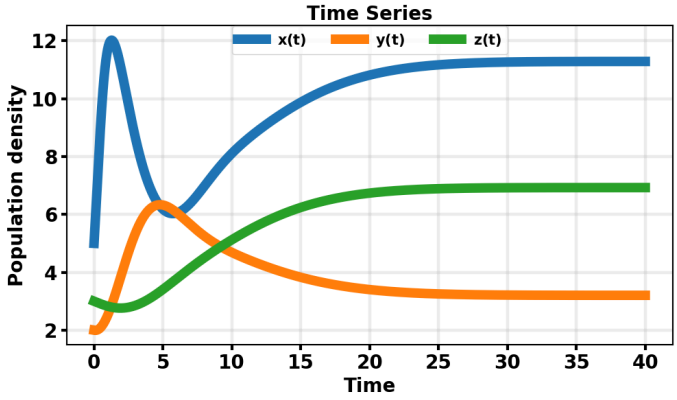
The numerical analysis was performed using the parameter set given in Table 2. The parameter values were adopted from previous studies where available, whereas several values were assumed

for the numerical investigation. The cited studies provide reference values or biologically relevant parameter ranges; however, these values are not assumed to be directly transferable to the present model, because the referenced studies may differ in species, model structure, functional responses, and parameter definitions. Therefore, the literature-based values are used as representative values for the present mathematical analysis rather than as directly calibrated ecological parameters. Since the values were obtained from different studies and are not derived from a common empirical dataset, the parameter set is not intended to represent a quantitatively calibrated ecological system. Instead, it provides a consistent illustrative parameter regime for examining the dynamical properties and bifurcation behavior of the proposed mathematical model. Unless otherwise stated, the variables are expressed in generic population units and time is expressed in generic time units, with the parameters interpreted in the corresponding model-dependent units. Therefore, the resulting equilibrium and bifurcation values should be interpreted as dynamical properties of the proposed mathematical system under the selected parameter regime, rather than as quantitative predictions for a specific ecological population.

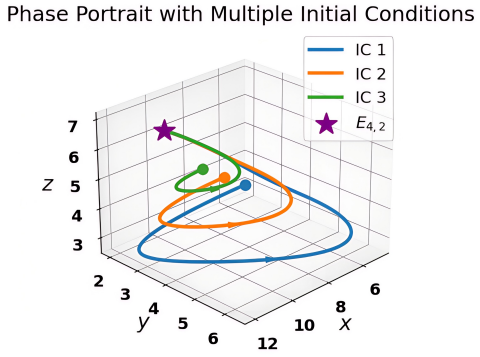
Table 2: Parameter values

Parameter	Value	Biological meaning	Reference
b	3.80	Intrinsic birth/growth rate of the prey	[13]
a	0.18	Intraspecific competition coefficient of the prey	Assumed
d	0.15	Natural mortality rate of the prey	[14]
α	0.15	Intensity of the fear effect	[15]
m_1	0.12	Predation rate of the middle predator	Assumed
e_1	0.60	Biomass conversion efficiency of the middle predator	[16]
d_1	0.12	Natural mortality rate of the middle predator	[17]
m_2	0.10	Predation rate of the top predator	[12]
e_2	0.50	Biomass conversion efficiency of the top predator	[18]
γ	1.00	Allee-effect scale parameter	[19]
d_2	0.14	Natural mortality rate of the top predator	Assumed

The equilibrium system in Eq. (2) admits two biologically feasible positive coexistence equilibria, $E_{4,1} = (2.30691511,\ 8.87403103,\ 0.46097888)$ and $E_{4,2} = (11.28881211,\ 3.20416027,\ 6.92794472)$. Both equilibria satisfy $x^*, y^*, z^* > 0$. Their Jacobian eigenvalues are $E_{4,1}$: $\lambda_{1,2} = -0.20330231 \pm 0.54061569i$ and $\lambda_3 = 0.08718606$, whereas $E_{4,2}$: $\lambda_1 = -1.32247438$ and $\lambda_{2,3} = -0.34592637 \pm 0.12707197i$. Hence, $E_{4,1}$ is unstable, whereas $E_{4,2}$ is locally asymptotically stable. These results are consistent with the Routh–Hurwitz analysis.



(a) Time-series dynamics of (x), (y), and (z).



(b) Three-dimensional phase portrait for multiple initial conditions.

Fig. 1: Numerical dynamics of the three-species system showing convergence toward the stable coexistence equilibrium $E_{4,2}$.

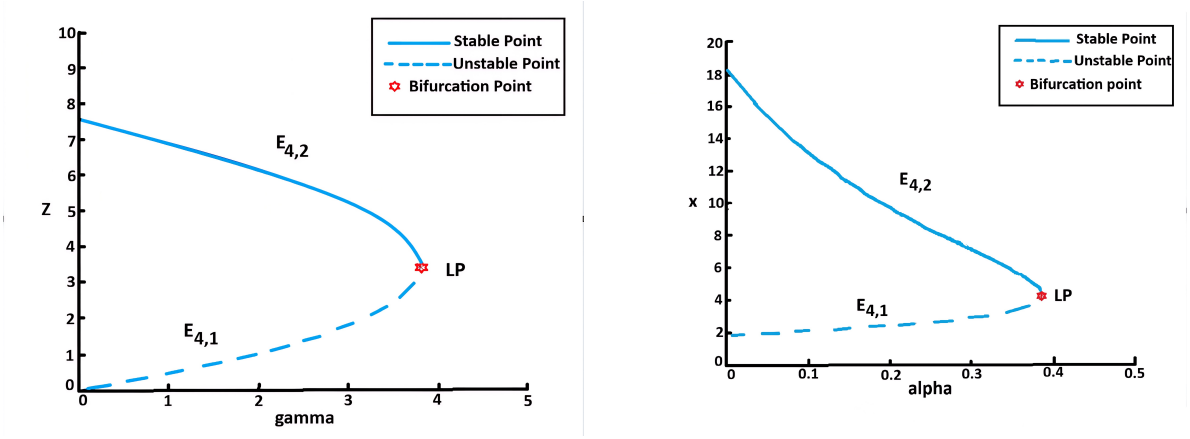
The numerical trajectories were obtained using RK45 with rtol $= 10^{-9}$ and atol $= 10^{-11}$. Figure 1a shows the time-series dynamics from the initial condition $(x(0), y(0), z(0)) = (5, 2, 3)$

over $0 \leq t \leq 40$. The populations exhibit transient oscillations before approaching $E_{4,2}$. Figure 1b presents the three-dimensional phase portrait for the initial conditions $(5, 2, 3)$, $(7, 2.5, 4)$, and $(9, 3, 5)$ over $0 \leq t \leq 150$. Although the trajectories have different transient paths, they approach the same positive coexistence equilibrium $E_{4,2}$, consistent with its locally asymptotically stable character. These simulations support the local stability result but do not establish global asymptotic stability.

3.5. Bifurcation Analysis

The bifurcation behavior of the system in Eq. (1) was investigated using MATCONT through one-parameter equilibrium continuation. The Allee-effect parameter γ and fear-effect parameter α were varied separately while the remaining parameters were fixed. The initial, minimum, and maximum step sizes were 0.01, 10^{-5}, and 0.1, respectively, with adaptation parameter 3 and 300 maximum continuation points. Closed-branch checking was performed every 50 points. The Newton correction used at most 3 Newton iterations, 10 correction iterations, and 10 test iterations, with variable, function, and test tolerances of 10^{-6}, 10^{-6}, and 10^{-5}, respectively. The Jacobian increment was 10^{-5}, with TSearch order and Moore–Penrose options enabled. Critical points were detected from Jacobian singularities, with a limit point (LP) corresponding to a fold (saddle-node) bifurcation of the equilibrium branch and characterized by a simple zero eigenvalue.

3.5.1. Limit Point Bifurcations Induced by Allee and Fear Effects



(a) Limit point bifurcation induced by the Allee effect (γ).

(b) Limit point bifurcation induced by the fear effect (α).

Fig. 2: Limit point bifurcations induced by Allee and fear effects. Panel (a) shows the limit point bifurcation induced by the Allee effect (γ), while panel (b) shows the limit point bifurcation induced by the fear effect (α).

In Figure 2a, the Allee-effect parameter γ was varied as the single free parameter and the top-predator density z^* was used as the state variable. A limit point was detected at $\gamma_{\mathrm{LP}} = 3.799530$, with the corresponding equilibrium $(x, y, z, \gamma) = (6.469650, 5.876411, 3.458148, 3.799530)$. Numerical evaluation of the Jacobian at this point gives the eigenvalues $\lambda_1 = 0$ and $\lambda_{2,3} = -0.545622 \pm 0.659245i$. Thus, the zero eigenvalue is simple and the remaining eigenvalues have nonzero real parts. MATCONT reported the quadratic normal-form coefficient $a = -9.920180 \times 10^{-3} \neq 0$, supporting the nondegeneracy of the quadratic term at the detected limit point. The two positive coexistence branches $E_{4,1}$ and $E_{4,2}$ coalesce at this point, with $E_{4,1}$ unstable and $E_{4,2}$ stable away from the limit point. Thus, variation in γ produces a saddle-node structure in the positive coexistence equilibria.

Similarly, as shown in Figure 2b, varying the fear parameter α and tracking the prey density x^* yielded a limit point at $\alpha_{\mathrm{LP}} = 0.384437$, with $E_{\mathrm{LP}} = (4.337647, 4.255978, 1.923106)$.

The Jacobian eigenvalues at this point are $\lambda_1 = 0$ and $\lambda_{2,3} = -0.366442 \pm 0.542374i$. The corresponding quadratic normal-form coefficient was $a = -1.179004 \times 10^{-2} \neq 0$, supporting the nondegeneracy of the quadratic term. The positive coexistence branches $E_{4,1}$ and $E_{4,2}$ coalesce at the turning point, with their local stability determined from the Jacobian eigenvalues. Hence, variation in α also modifies the existence and stability of positive coexistence equilibria through a limit-point structure. These bifurcation results describe the dynamical behavior of the proposed mathematical system under the selected illustrative parameter regime and should not be interpreted as quantitative predictions for a specific ecological food chain.

3.5.2. Limit Point Bifurcations Induced by Middle-Predator Predation

Figure 3 shows the effect of m_1, representing the predation rate of the middle predator on the prey (x), investigated by continuation of the positive coexistence equilibrium branch. Two limit points were detected at $(x, y, z, m_1) = (8.808777, 6.175214, 0.829577, 0.038401)$ and $(2.228124, 3.184487, 7.282434, 0.634497)$, respectively. At the first limit point, the Jacobian eigenvalues are $\lambda_1 = 0$, $\lambda_2 = -1.416629$, and $\lambda_3 = -0.092430$, whereas at the second limit point they are $\lambda_1 = 0$ and $\lambda_{2,3} = -0.192079 \pm 1.573957i$. Thus, both points possess a simple zero eigenvalue with the remaining eigenvalues away from the imaginary axis. The corresponding quadratic normal-form coefficients were $a = -2.219361 \times 10^{-2} \neq 0$ and $a = -2.132606 \times 10^{-3} \neq 0$, respectively. These nonzero coefficients support the nondegeneracy of the quadratic term at both limit points. The continuation diagram shows the associated fold structure of the positive coexistence branch, with stable and unstable portions separated by the turning points. Thus, variation in m_1 produces two limit points and can change the number of positive coexistence equilibria under the selected parameter regime.

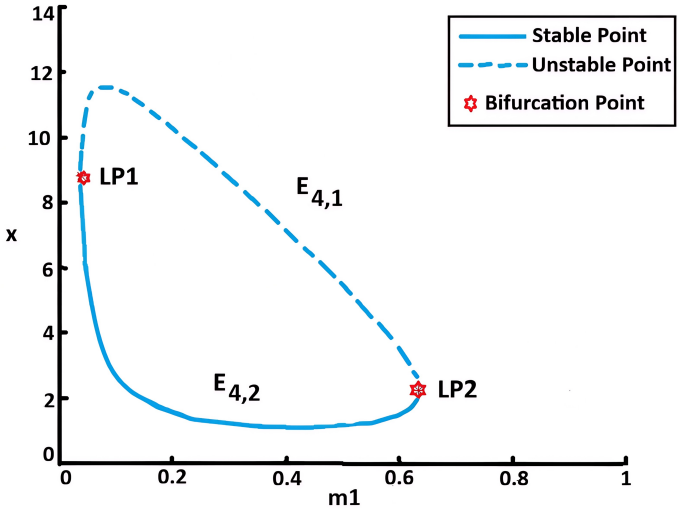


Fig. 3: Limit point bifurcations induced by predation rate of the middle predator (m_1) on the prey (x). The detected limit points occur at $m_1 = 0.038401$ and $m_1 = 0.634497$.

3.5.3. Bifurcations Induced by Top-Predator Predation

Figure 4 shows the effect of m_2, representing the predation rate of the top predator on the middle predator (y), investigated by continuing the positive coexistence equilibrium branch. One Hopf bifurcation and one limit point were detected. The Hopf point occurred at $(x, y, z, m_2) = (18.991899, 0.349857, 0.558636, 2.232969)$. Numerical evaluation of the Jacobian at this point gives the critical eigenvalues $\lambda_{1,2} = \pm 0.413713i$ and $\lambda_3 = -3.328720$. Thus, a purely imaginary conjugate pair is present while the third eigenvalue has negative real part. The transversality condition was verified numerically along the equilibrium branch, yielding $d\,\mathrm{Re}\,\lambda/dm_2|_{m_2=2.232969} = 0.0141491 \neq 0$,

where λ denotes the critical complex eigenvalue. Together with the first Lyapunov coefficient $l_1 = 3.836475 \times 10^{-4} > 0$, these results support the classification of the detected point as a subcritical Hopf bifurcation. The positive Lyapunov coefficient predicts a nearby unstable periodic orbit in the normal form. Since periodic-orbit continuation was not performed, this periodic orbit is not claimed as a numerically continued branch.

A limit point was detected at $(x, y, z, m_2) = (3.964817, 7.600139, 3.491324, 0.047394)$. The Jacobian eigenvalues at this point are $\lambda_1 = 0$ and $\lambda_{2,3} = -0.341249 \pm 0.644091i$. Thus, the point has a simple zero eigenvalue with the remaining eigenvalues having negative real parts. The quadratic normal-form coefficient was $a = -6.483749 \times 10^{-3} \neq 0$, supporting the nondegeneracy of the quadratic term at the detected limit point. The continuation diagram shows a stable positive coexistence branch between the limit point and Hopf point, followed by an unstable branch after the Hopf bifurcation. Hence, variation in m_2 produces both a limit-point structure affecting the number of positive coexistence equilibria and a subcritical Hopf bifurcation affecting their local stability under the selected parameter regime.

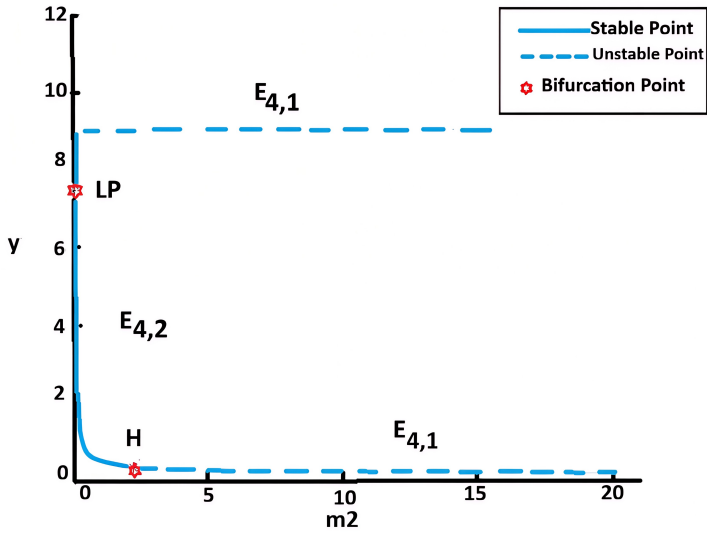


Fig. 4: Bifurcation diagram with respect to the predation rate of the top predator (m_2) on the middle predator (y). The limit point bifurcation occurs at $m_2 = 0.047394$, while the Hopf bifurcation occurs at $m_2 = 2.232969$.

4. Conclusion

This study investigated a three-species system incorporating predator-induced fear in the prey and an Allee effect in the top predator, focusing on coexistence equilibria, local stability, and bifurcations. Multiple biologically feasible coexistence equilibria were shown to occur under the same parameter regime with different stability properties, while numerical simulations confirmed convergence to the locally asymptotically stable coexistence state. MATCONT continuation showed that variation in the Allee-effect scale parameter γ and fear parameter α can induce limit point bifurcations and alter the equilibrium structure. Variation in m_1 produced two limit points, indicating multiple saddle-node transitions and changes in the number of positive coexistence equilibria, whereas variation in m_2 produced a limit point and a subcritical Hopf bifurcation, indicating both equilibrium transitions and changes in local stability. These results demonstrate that the considered interaction parameters can substantially influence the dynamical behavior of the system under the selected parameter regime. The equilibrium analysis, Routh–Hurwitz criteria, numerical simulations, and MATCONT continuation provide a systematic framework for identifying equilibrium and oscillatory transitions in the proposed mathematical system. The parameter set used in this study is illustrative rather than calibrated to a specific ecological

food chain; therefore, the reported bifurcation values should be interpreted within the selected mathematical parameter regime rather than as quantitative ecological predictions. Future work may extend this analysis to two-parameter bifurcations and broader parameter regimes to explore the interactions among fear, Allee effects, and predation rates. The basin structure associated with the stable coexistence equilibrium and the possible attraction toward boundary or extinction states were not systematically investigated and constitute a direction for future work.

CRediT Authorship Contribution Statement

Dana Eky Novya: Conceptualization, Methodology, Software, Formal Analysis, Investigation, Writing–Original Draft, Visualization. **Dian Savitri:** Conceptualization, Methodology, Validation, Writing–Review & Editing, Visualization, Supervision.

Declaration of Generative AI and AI-assisted technologies

During the development of this study, the authors used ChatGPT to assist with manuscript organization, initial drafting, and language refinement. The authors reviewed and revised the generated content and take full responsibility for the final manuscript.

Declaration of Competing Interest

The authors declare no competing interests.

Ethics Approval and Consent to Participate

Ethics approval was not required for this study.

Funding and Acknowledgments

The authors sincerely thank their supervisor for valuable guidance and support throughout the research, and their colleagues for their assistance and contributions to this manuscript.

Data and Code Availability

The Python codes for numerical simulations and the MATCONT files for numerical continuation and bifurcation analysis can be accessed through the following GitHub repository: https://github.com/dynamicstism/Dynamic-Analysis-of-Three-Species-System-with-Fear-Effect-on-Prey-and-Allee-Effect-on-Top-Predator.git.

References

[1] Pijush Panday, Sudip Samanta, Nikhil Pal, and Joydev Chattopadhyay. “Delay induced multiple stability switch and chaos in a predator–prey model with fear effect”. In: *Mathematics and Computers in Simulation* 172 (2020), pp. 134–158. DOI: 10.1016/j.matcom.2019.12.015.

[2] Pingping Cong, Meng Fan, and Xingfu Zou. “Dynamics of a three-species food chain model with fear effect”. In: *Communications in Nonlinear Science and Numerical Simulation* 99 (2021), p. 105809. DOI: 10.1016/j.cnsns.2021.105809.

[3] Binfeng Xie. “Impact of the fear and Allee effect on a Holling type II prey–predator model”. In: *Advances in Difference Equations* 2021 (2021), p. 464. DOI: 10.1186/s13662-021-03592-6.

[4] Soumitra Pal, Pankaj Kumar Tiwari, Arvind Kumar Misra, and Hao Wang. "Fear effect in a three-species food chain model with generalist predator". In: *Mathematical Biosciences and Engineering* 21.1 (2024), pp. 1–33. DOI: 10.3934/mbe.2024001.

[5] Ying Huang, Zhenliang Zhu, and Zhong Li. "Modeling the Allee effect and fear effect in predator–prey system incorporating a prey refuge". In: *Advances in Difference Equations* 2020 (2020), p. 321. DOI: 10.1186/s13662-020-02727-5.

[6] Udai Kumar and Partha Sarathi Mandal. "Role of Allee effect on prey–predator model with component Allee effect for predator reproduction". In: *Mathematics and Computers in Simulation* 193 (2022), pp. 623–665. DOI: 10.1016/j.matcom.2021.10.027.

[7] S. Vinoth, R. Sivasamy, K. Sathiyanathan, Grienggrai Rajchakit, P. Hammachukiattikul, R. Vadivel, and Nallappan Gunasekaran. "Dynamical analysis of a delayed food chain model with additive Allee effect". In: *Advances in Difference Equations* 2021 (2021), p. 54. DOI: 10.1186/s13662-021-03216-z.

[8] Liyun Lai, Zhenliang Zhu, and Fengde Chen. "Stability and Bifurcation in a Predator–Prey Model with the Additive Allee Effect and the Fear Effect". In: *Mathematics* 8.8 (2020), p. 1280. DOI: 10.3390/math8081280.

[9] Yajing Li, Mengxin He, and Zhong Li. "Dynamics of a ratio-dependent Leslie–Gower predator–prey model with Allee effect and fear effect". In: *Mathematics and Computers in Simulation* 201 (2022), pp. 417–439. DOI: 10.1016/j.matcom.2022.05.017.

[10] Changcheng Ke, Ming Yi, and Yanfeng Guo. "Qualitative Analysis of a Spatiotemporal Prey–Predator Model with Additive Allee Effect and Fear Effect". In: *Complexity* 2022 (2022), p. 5715922. DOI: 10.1155/2022/5715922.

[11] Sourav Rana, Sabyasachi Bhattacharya, and Sudip Samanta. "Complex Dynamics of a Three-Species Food Chain Model with Fear and Allee Effect". In: *International Journal of Bifurcation and Chaos* 32.6 (2022), p. 2250084. DOI: 10.1142/S0218127422500845.

[12] Vinay Kumar, Suneel Kumar Bairwa, and Tanvi. "Influence of fear and Allee effects on stability and species survival in a tri-trophic food chain". In: *Communications in Nonlinear Science and Numerical Simulation* 152 (2026), p. 109115. DOI: 10.1016/j.cnsns.2025.109115.

[13] Debasis Mukherjee. "Dynamics of A Discrete-Time Ecogenetic Predator-Prey Model". In: *Communication in Biomathematical Sciences* 5.2 (2022), pp. 161–169. DOI: 10.5614/cbms.2022.5.2.5.

[14] Subarna Roy and Pankaj Kumar Tiwari. "Bistability in a Predator–Prey Model Characterized by the Crowley–Martin Functional Response: Effects of Fear, Hunting Cooperation, Additional Foods and Nonlinear Harvesting". In: *Mathematics and Computers in Simulation* 228 (2025), pp. 274–297. DOI: 10.1016/j.matcom.2024.09.001.

[15] Xinyu Meng, Lijuan Chen, and Fengde Chen. "Dynamics of a Predator–Prey System with Asymmetric Dispersal and Fear Effect". In: *Symmetry* 17.3 (2025), p. 329. DOI: 10.3390/sym17030329.

[16] Jake M. Ferguson, John B. Hopkins III, and Briana H. Witteveen. "Integrating Abundance and Diet Data to Improve Inferences of Food Web Dynamics". In: *Methods in Ecology and Evolution* 9.6 (2018), pp. 1581–1591. DOI: 10.1111/2041-210X.13001.

[17] Anna Kuparinen and Jeffrey A. Hutchings. "Increased Natural Mortality at Low Abundance Can Generate an Allee Effect in a Marine Fish". In: *Royal Society Open Science* 1.2 (2014), p. 140075. DOI: 10.1098/rsos.140075.

[18] Karin A. Nilsson, Kevin S. McCann, and Amanda L. Caskenette. "Interaction Strength and Stability in Stage-Structured Food Web Modules". In: *Oikos* 127.10 (2018), pp. 1494–1505. DOI: 10.1111/oik.05029.

[19] Shuangte Wang and Hengguo Yu. "Complexity Analysis of a Modified Predator-Prey System with Beddington–DeAngelis Functional Response and Allee-Like Effect on Predator". In: *Discrete Dynamics in Nature and Society* 2021 (2021), p. 5618190. DOI: 10.1155/2021/5618190.